Preprints of the 19th World Congress
The International Federation of Automatic Control
Cape Town, South Africa. August 24-29, 2014

Coordinated contribution of wind turbines to frequency regulation by model predictive control

F. Baccino * **F. Conte** * **S. Grillo** ** **S. Massucco** * **F. Silvestro** *

* *Dipartimento di Ingegneria Navale, Elettrica, Elettronica e delle Telecomunicazioni, Università degli Studi di Genova, via all'Opera Pia, 11A , I-16145 Genova (GE), Italy (e-mail: {francesco.baccino; fr.conte; stefano.massucco; federico.silvestro}@unige.it)*
** *Dipartimento di Elettronica, Informazione e Bioingegneria, Politecnico di Milano, via Ponzio 34/5, I-20133 Milano, Italy (e-mail: samuele.grillo@polimi.it)*

Abstract: This work proposes an innovative control technique for improving the contribution to the grid frequency regulation provided by a set of wind power generators belonging to a wind farm. Models of individual generators and of the conventional grid primary frequency control are developed and used for designing a model predictive controller. A proper estimation algorithm is also introduced in order to provide both the dynamical state of the wind turbines and the actual local wind conditions to the regulator. The availability of this data makes the control algorithm able to improve the participation of the whole wind farm to the frequency regulation by suitably coordinating and differentiating the contribution of the individual generators. The proposed strategy is tested on a large wind farm using a dedicated real-time/real-data simulation environment.

Keywords: Electric power systems; Predictive control; Optimal control; Power generation; Wind generation

1. INTRODUCTION

In the last decades, with the wide development of renewable energy sources (RESs), the intelligent control of power systems has acquired great relevance (Venkat et al. [2008], Menichelli and Bemporad [2008], Zong et al. [2012]). RESs may indeed induce disturbances due both to their intrinsic randomness and to possible structural weaknesses of the grid precisely where large RESs farms are connected to the grid (Grillo et al. [2010b, 2012]). Anyway, the increased penetration of RESs opens to their possible contribution to ancillary services provision in order to ensure power system stability and reliability. The grid frequency regulation is one of the most important among these services. Wind power has not historically been required to provide this kind of service. However, due to the large penetration today large-scale wind farms (WFs) can reasonably contribute to the frequency support (Rahmann et al. [2011], Ramtharan et al. [2009], Xiang et al. [2006], Aho et al. [2012]).

Many control techniques have been proposed to achieve these results. The most used strategy is known as kinetic energy control (KEC) (e.g. de Almeida and Peças Lopes [2007], Erlich and Wilch [2010], Grillo et al. [2010a]). The main drawback of these techniques is the inability to adapt the reaction of the wind turbines (WTs) to the frequency variation, in function of their current dynamical conditions. In fact, as shown in Muljadi et al. [2012], the capability of a WT in supporting the grid frequency changes with wind speed. As a consequence, an intelligent control should differentiate the power delivery based on the wind conditions which, in a large-scale WF may significantly differ among sufficiently far WTs.

The aim of this work is to design a control strategy able to coordinate the frequency support provided by each WT taking into account the specific capability of power delivery due to different wind conditions. This is obtained by introducing a model predictive control (MPC) algorithm (Mayne et al. [2000]) which, when activated, modifies the operating point of each WT according to an optimization criterion. It is therefore needed an algorithm able to estimate the local wind conditions, allowing the regulator to suitably define the contribution to frequency regulation of each wind generator.

The paper is organized as follows. Section 2 describes the mathematical models required by the control algorithm, which is detailed in Section 3. Section 4 shows the simulation results. Finally, Section 5 summarizes the conclusions of the paper.

2. MODELS OF WIND TURBINES AND FREQUENCY CONTROL

The aim of the paper is to determine the contribution to the frequency regulation of a set of N variable-speed WTs composing a WF. They are connected to the main

grid, where the conventional *primary frequency control* is operated. Frequency basically depends on the (active) power balance. A power source, such as a WT, can tough contribute to keep the frequency close to its nominal value by suitably varying the power delivery when a frequency variation occurs. The principal control objective here is to establish this power variation for each of the N WTs within the WF. As a consequence, on the WF side, the impact of a given variation of power delivery to the dynamical state of the WTs has to be modelled; whereas, on the main grid side, a model representing the impact of a variation in the WF power delivery to the grid frequency is required. Such models are introduced in this section.

2.1 Variable-Speed Wind Turbines Model

As depicted in Fig. 1, a full converter variable-speed WT generally consists of four main components: the rotating blades (also referred to as rotor), which capture the aerodynamic power $P_{a,i}$; the shaft, that transmits the captured power; the generator, which converts the available power from the mechanical to the electric form; and the converter which determines the power delivered to the grid $P_{ref,i}$, and, consequently, the electro-mechanic torque $T_{g,i}$. For all the considered quantities, the subscript i indicates the i-th WT within the WF.

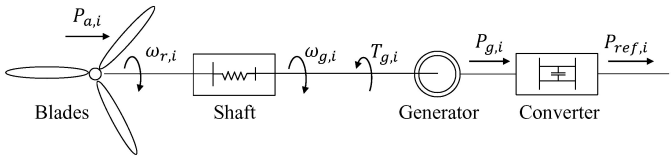

Fig. 1. Schematic representation of a full converter variable-speed wind turbine generator.

The dynamic of a WT can be summarized by the following model (Aho et al. [2012]):

$$\dot{\omega}_{r,i} = \frac{1}{J_r}\left(\frac{P_{a,i}}{\omega_{r,i}} - \mu\theta_{d,i} - \kappa\left(\omega_{r,i} - \omega_{g,i}\right)\right), \tag{1}$$

$$\dot{\omega}_{g,i} = \frac{1}{J_g}\left(\mu\theta_{d,i} + \kappa\left(\omega_{r,i} - \omega_{g,i}\right) - \frac{P_{g,i}}{\omega_{g,i}}\right), \tag{2}$$

$$\dot{\theta}_{d,i} = \omega_{r,i} - \omega_{g,i}, \tag{3}$$

where $\omega_{r,i}$ and $\omega_{g,i}$ are the blades and generator angular speeds $[rad/s]$, respectively, J_r and J_g are the rotor and generator inertia $[kg \cdot m^2]$, respectively, $\theta_{d,i}$ is the shaft deformation angle $[rad]$, μ is the shaft elastic constant $[kg \cdot m^2/s^2]$, and κ is the damping coefficient $[kg \cdot m^2/s]$. The system state is driven by the aerodynamic torque $T_{a,i} = P_{a,i}/\omega_{r,i}$ and the electro-mechanic torque $T_{g,i} = P_{g,i}/\omega_{g,i}$. The former depends on the aerodynamic power $P_{a,i}$, the latter depends on the generator power $P_{g,i}$, which is regulated by the converter.

The power captured by the rotating blades is given by

$$P_{a,i} = \frac{1}{2}\rho\pi R^2 C_p(\beta_i, \lambda_i) v_i^3, \qquad \lambda_i = \frac{\omega_{r,i} R}{v_i}, \tag{4}$$

where ρ is the air density $[kg/m^3]$, R is the rotor radius $[m]$, v_i is the speed of the wind component perpendicular to rotor plane $[m/s]$, β_i is the pitch angle $[deg]$, and λ_i is the so called tip-speed ratio (TSR). The power coefficient C_p is an aerodynamic characteristic of the blades' profiles.

The generator power $P_{g,i}$ is regulated by the converter, driven by a reference signal $P_{ref,i}$ which coincides with the instantaneous power delivered to the grid. Because the dynamic of the converter is significantly faster than the mechanical one, the converter is supposed to be ideal, so that $P_{g,i} = P_{ref,i}$ (Erlich and Wilch [2010], Ma and Chowdhury [2010]). This means that the converter allows the user to instantly determine the delivered power $P_{g,i}$ and, consequently, the electro-mechanic torque $T_{g,i}$.

Finally, the total power delivered by the WF to the grid is

$$P_w = \sum_{i=1}^{N} P_{g,i}. \tag{5}$$

2.2 Power Network Primary Frequency Control Model

The primary frequency control is a fundamental task generally operated by conventional generators which are called to limit any frequency variation due to power unbalances. The control goal is not to bring back the frequency to its nominal value—which is required to the secondary control—but to only limit the variation to keep the secure grid operating conditions. The standard control strategy is known as *frequency droop control* by which the generators limit the frequency variation with a final *droop* $\Delta f/f^{nom} = -k_p(\Delta P/P^{nom})$, where ΔP is the grid power variation$[W]$, k_p is the *droop ratio*, f^{nom} is the nominal frequency $[Hz]$, and P^{nom} is the nominal power of the generator $[W]$. More specifically, the regulation typically acts with a 0-type response to an external power variation (Saccomanno [2003]), i.e.

$$\frac{\Delta f(s)}{\Delta P(s)} = -\frac{1}{k_f}\frac{\tau s + 1}{\frac{s^2}{\omega_n^2} + 2\frac{\zeta}{\omega_n}s + 1}, \tag{6}$$

where k_f^{-1} is the steady state gain ($k_f^{-1} = k_p f^{nom}/P^{nom}$). A possible approach for identifying the parameters of (6) is shown in Bruno et al. [2006]. By assuming the system stability, a state-space realization can be readily derived from (6):

$$\dot{\Delta f} = \Delta f - a_1 x_f + b_1 \Delta P, \tag{7}$$

$$\dot{x}_f = -a_0 x_f + b_0 \Delta P, \tag{8}$$

where x_f is an auxiliary state variable.

The total grid power variation can be expressed as $\Delta P = \Delta P_L - \Delta P_w$, where $\Delta P_w = \sum_i \Delta P_{g,i}$ is the total variation of power provided by the WF and ΔP_L is the total external power load variation.

3. CONTROL STRATEGY

The control architecture proposed in this paper is depicted in Fig. 2. There are two levels of regulation: the local control has to administrate a WT during the normal operating conditions; the central control has to activate and coordinate the contribution to the frequency regulation of all the WTs, when a significant power unbalance occurs into the grid.

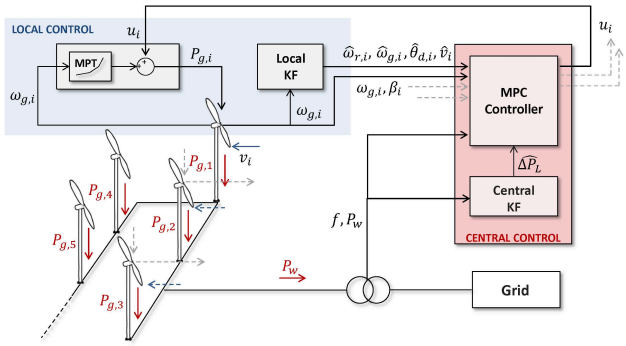

Fig. 2. Control architecture.

The local control operates a conventional maximum power tracking (MPT) regulation by using a look-up table that defines the optimal power $P_{g,i}$ to be delivered to the grid for a given value of the measured generator speed $\omega_{g,i}$, i.e. $P_{g,i} = P^*_{g,i}(\omega_{g,i})$. In the same time, it monitors the dynamic condition of the WT by estimating the system state $(\omega_{r,i}; \omega_{g,i}; \theta_{d,i})$ and the wind speed v_i. A proper Kalman filter (named *Local KF* in Fig. 2) is used for obtaining such estimates. Finally, the pitch angle β_i is assumed to be independently determined by standard proportional-integral (PI) regulators which keep $\omega_{g,i}$ and $P_{g,i}$ under their nominal values.

The central controller receives from each of the WTs the estimated dynamical state and wind speed and the sampled measurements of $\omega_{g,i}$ and β_i. Moreover, it receives the measurements of Δf and P_w from the point of common coupling (PCC). Based on these information, the controller has to determine the variation u_i from the local MPT signal $P^*_{g,i}$ in order to contribute to the frequency primary regulation. The resulting control input for the WTs has the following form:

$$P_{g,i} = P^*_{g,i}(\omega_{g,i}) + u_i. \tag{9}$$

The variation u_i is determined by an MPC algorithm which uses all the mentioned information and the estimate of the unknown total external load $\Delta\hat{P}_L$. This last is computed by a Kalman Filter, named *Central KF* in Fig. 2. The use of this estimate will be made clearer in the following.

3.1 Local Kalman Filter

The local KF has to estimate the dynamical state of the WT and the wind speed. Despite the fact that wind power generators are usually equipped with anemometers, the use of direct wind measurements for estimation is not preferable. This is due to the presence of aerodynamic turbulent phenomena, caused by the turbine rotating blades, and the difference between the wind measured by anemometers and the component that transfers the power to the rotor. As a consequence, the wind estimation must be carried out exploiting the indirect information given by the dynamical state of the considered WT which is also required by the MPC algorithm.

The main difficulties of this method are due to the nonlinear nature of the dynamical model (1)-(3), that requires the introduction of approximations.

Some literature approaches (Qiao et al. [2008]) propose a linear estimation of the rotor mechanical torque $T_{a,i}$, followed by the numeric solution of the nonlinear equation $T_{a,i} = P_{a,i}(\omega_{r,i}, v_i, \beta_i)/\omega_{r,i}$. This may represent a drawback for real applications from the computational point of view. The idea of the filtering solution proposed in the following is to obtain a recursive estimation procedure and reduce as much as possible the significance of the above approximations.

Let us define the extended state vector

$$z_i = [\, \omega_{r,i} \;\; \dot{\omega}_{r,i} \;\; \omega_{g,i} \;\; \theta_{d,i} \;\; v_i \,]^T, \tag{10}$$

which, taking into account (1)-(3), is governed by the dynamic model

$$\dot{z}_{i,1} = z_{i,2}, \tag{11}$$
$$\dot{z}_{i,2} = \sigma_\omega w_{i,1}, \tag{12}$$
$$\dot{z}_{i,3} = \frac{1}{J_g}\left(\kappa\left(z_{i,1} - z_{i,3}\right) + \mu z_{i,4}\right) - \frac{1}{J_g}\frac{P_{g,i}}{z_{i,3}}, \tag{13}$$
$$\dot{z}_{i,4} = z_{i,1} - z_{i,3}, \tag{14}$$
$$\dot{z}_{i,5} = \sigma_v w_{i,2}, \tag{15}$$

where $w_i \in \mathbb{R}^2$ is a standard zero-mean Gaussian white-noise process. Two equations have been added with respect to (1)-(3). The former (12) is the time derivative of the rotor angular acceleration $\dot{\omega}_{r,i}$; the latter (15) is the time derivative the wind speed v_i. Both of them are supposed to be independent Gaussian white random processes with standard variations σ_ω and σ_v, respectively. Equation (12) has been added in order to make the filter able to estimate the rotor angular acceleration. This allows the filtering process to use the rotor dynamical balance (1) as an output equation, as shown in the following. This choice has been made for avoiding the zero-holding of such a strongly nonlinear differential equation. Equation (15) has been added in order to make the filter able to estimate the wind speed. Finally note that the quantity $P_{g,i}$ is completely known by (9) and that the term $P_{g,i}/z_{i,3}$ constitutes the unique nonlinearity of the state equations (11)-(15).

Two measurements are available for system (11)-(15). The first one is the generator angular speed $\omega_{g,i} = z_{i,3}$. The second one is the rotor dynamical balance (1) which must be identically equal to zero. Therefore, the output vector $y_i = [\, y_{i,1} \;\; y_{i,2} \,]^T$ is composed by

$$y_{i,1} = \omega_{g,i} + n_{\omega_g,i}, \tag{16}$$
$$y_{i,2} = n_{m,i}, \tag{17}$$

where $n_{\omega_g,i}$ and $n_{m,i}$ are independent Gaussian white processes with standard variations σ_{ω_g} and σ_m which model the measurement error of the generator angular speed and the model error in the dynamic balance (1), respectively. The output vector y_i is related to the state vector (10) by the following output map:

$$y_{i,1} = z_{i,3} + n_{\omega_g,i}, \tag{18}$$
$$y_{i,2} = -\frac{1}{J_r}\left(\frac{P_{a,i}}{z_{i,1}} - \mu z_{i,4} - \kappa\left(z_{i,1} - z_{i,3}\right)\right) + z_{i,2} + n_{m,i}. \tag{19}$$

The system described by (11)-(15) and (18)-(19) is discretized by zero-holding, with sampling time T_s^f, which introduces approximations only because of the forcing term $P_{g,i}/z_{i,3}$. The discretized model can be finally used to implement a state estimation algorithm by applying the standard extended Kalman filter (EKF).

3.2 Central Kalman Filter

Model (7)–(8) can be rewritten and extended as follows:

$$\dot{\Delta f} = \Delta f - a_1 x_f + b_1 \Delta P_L - b_1 \Delta P_w \tag{20}$$

$$\dot{x}_f = -a_0 x_f + b_0 \Delta P_L - b_0 \Delta P_w \tag{21}$$

$$\dot{\Delta P_L} = w_{P_L} \tag{22}$$

$$y_f = \Delta f + n_f \tag{23}$$

where w_{P_L} and n_f are independent Gaussian white-noise process, with standard variation σ_{P_L} and σ_f, respectively, y_f is the available measurement and ΔP_w is a completely known quantity. Since the resulting system is linear, it can be exactly discretized, with sampling time T_s^f and a standard KF algorithm can be used to estimate the state, which contains the required quantity ΔP_L. Obviously, since ΔP_w is known, the estimate $\hat{\Delta P} = \hat{\Delta P_L} - \Delta P_w$ is available as well.

3.3 Central control algorithm

The central control consists into two tasks: 1) the *model update*, during which the system model is updated with a given sampling time T_s^{up} and no control variation is transmitted to the WTs (i.e. $u_i = 0,\ \forall i = 1, 2, \ldots, N$); 2) the *MPC frequency support*, during which a proper MPC algorithm determines the contribution of each WT to the frequency control. These two tasks are detailed in the next, followed by the *scheduling strategy* used for activate and deactivate the MPC frequency support.

Model update: The WT model (1)-(3) can be approximated by linearization. The state variables are the variations $\delta\omega_{r,i}$, $\delta\omega_{g,i}$, and $\delta\theta_{d,i}$ from the steady-state values at which the linearization is computed. They are collected into the vector

$$x_i = \left[\, \delta\omega_{r,i} \ \delta\omega_{g,i} \ \delta\theta_{d,i} \,\right]^T. \tag{24}$$

Assuming the changes of wind speed to be significantly slower than the mechanical dynamic, the steady-state values can be assumed to be $\bar{\omega}_{r,i} = \bar{\omega}_{g,i}$ equal to the measured $\omega_{g,i}$ and $\bar{\theta}_{d,i} = P^*_{g,i}(\bar{\omega}_{g,i})/(\mu\bar{\omega}_{g,i})$. Moreover, $\bar{\beta}_i$ is equal to the current measured β_i and $\bar{v}_i$ is assumed to be equal to the current estimate $\hat{v}_i$. The wind conditions are taken into account in the linearization when the nonlinear term $P_{a,i} = P_{a,i}(\omega_{r,i}, v_i)$ is differentiated.

Because of the control input (9), the variation of the total power provided by the WF ΔP_w assumes the following form:

$$\Delta P_w = \sum_{i=1}^{N} \Delta P_{g,i} = \sum_{i=1}^{N} \left(P^*_{g,i}(\omega_{g,i}) + u_i - P^*_{g,i}(\omega^0_{g,i}) \right)$$

where $\omega^0_{g,i}$ is the generator angular speed at the control initialization. Last equation makes the power plant model (20)-(21) nonlinear with respect to $\omega_{g,i}$. Therefore, (20)-(21) must be linearized at $\bar{\Delta f} = 0$, $\bar{x}_f = 0$ and $\omega_{g,i} = \bar{\omega}_{g,i}$.

The linearized models of the WTs and the controlled grid frequency dynamic are finally included in a unique model with the following state and control vectors

$$x = \left[\, x_1^T \ x_2^T \ \cdots \ x_N^T \ \delta f \ \delta x_f \,\right]^T,$$

$$u = \left[\, u_1 \ u_2 \ \cdots \ u_N \,\right]^T.$$

Such a model gives a complete representation of the dynamics of the quantities to be controlled. After a zero-hold discretization, with sampling time T_s^c, the model can be rewritten in the standard discrete-time linear form

$$x(k+1) = Ax(k) + Bu(k) + Md(k), \tag{25}$$

where $x(k)$, $u(k)$, and $d(k)$ indicate the sampled state variables, control inputs and unknown disturb vectors, respectively. Vector $d(k)$ actually is equal to the scalar quantity ΔP_L at the sampling time kT_s^c. Note that the filtering procedures described in Sections 3.1 and 3.2 provide the estimates of both the state $x(k)$ and the disturb $d(k)$. Equation (25) is the model to be updated at any time step kT_s^{up}.

MPC frequency support: The system representation (25) is amenable for applying an MPC solution to the main problem of this work: to contribute to the frequency control with a short-term action ($\sim 50 \div 80s$), maintaining secure conditions and recovering the optimal power delivery after the support phase. For obtaining this, the MPC solution to the *tracking problem* can be used. This algorithm allows to track an output reference signal $y^0(k)$ by optimizing a proper cost function at each sampling time and using the receding horizon principle (Mayne et al. [2000]). The output signal is related to the state vector by the linear map $y(k) = Cx(k)$.

In the particular case of this work the controlled variables selected through matrix C are all state variables except for δx_f, which has not physical meaning. The reference signal $y^0(k)$ is identically equal to zero for the dynamical WTs' states. As far as the frequency reference signal is concerned, in nominal conditions, the equilibrium point to be reached should be $\Delta f = 0$. However, when a power unbalance occurs, the primary frequency control is asked to drive the frequency variation to the droop $\Delta f = -k_p(\Delta P/P^{nom})f^{nom}$ (see Section 2.2). Therefore, the frequency reference signal is dynamically set to

$$\Delta f^0 = -k_p \frac{\hat{\Delta P_L} - \Delta P_w}{P^{nom}} f^{nom} \tag{26}$$

where the estimate $\hat{\Delta P_L}$ is provided by the central KF described in Section 3.2.

MPC allows the control to introduce optimization constraints for assure structural stability and secure operational conditions. In the particular case of this paper, the following constraints are included:

$$\begin{aligned} \omega_r^{cut-in} \le \omega_{r,i} \le \omega^{nom}, \qquad & \omega_r^{cut-in} \le \omega_{g,i} \le \omega^{nom}, \\ u^{min} \le u_i \le u^{max}, \qquad & -\theta_d^{max} \le \theta_{d,i} \le \theta_d^{max}, \\ -\Delta u^{max} \le u_i(k) - u_i(k-1) \le \Delta u^{max}, & \end{aligned}$$

where ω_r^{cut-in} is the cut-in angular speed, Δu^{max} is the maximum control variation between two sampling times, and θ_d^{max} is the maximal shaft torsion.

Scheduling strategy: The model update, as well as the filtering procedures, are always active. The MPC frequency support is activated and deactivated through the following rules. When the MPC is inactive, if $|\Delta f - \Delta f^0|$ is lower than the *activation threshold* Δf_{th}^a, the MPC frequency support is kept inactive; otherwise, it is activated. When the MPC is active, if $|\Delta f - \Delta f^0|$ is greater than the *deactivation threshold* $\Delta f_{th}^d < \Delta f_{th}^a$, the MPC frequency support is kept active; otherwise, it is deactivated. The use of a double threshold strategy allows the control system to avoid the activation chattering and sharp control variations.

4. SIMULATION RESULTS

In order to validate the proposed control strategy, a simulated field is implemented using the DIgSILENT Powerfactory platform (GmbH [2013]). The system is composed by: a wind farm, made up of twenty 2 MW-rated wind turbines equipped with full converter and permanent magnets synchronous generator (PMSG); the main grid, represented by an equivalent 1000 MVA steam power generator, which operates a 5% droop primary frequency control; and an external load whose power absorption is set to 600 MW and changed during the execution time for simulating power unbalances. The MPC control algorithm is implemented using the Matlab environment. The communication between the simulated field and the controller is realized through an Open Platform Communication (OPC) link.

All simulations are carried out in real-time modality. The measurements are sent from the simulated field to the controller every 0.2 seconds. Therefore, the local and central Kalman filters, described in Sections 3.1 and 3.2, operate with the sapling time $T_s^f = 0.2\ s$. When active, the MPC control signal is computed and sent to the simulated wind turbines with the sampling time $T_s^c = 1\ s$. The update sampling time is $T_s^{up} = 1\ s$. The activation and deactivation thresholds are $\Delta f_{th}^a = 0.1\ Hz$ and $\Delta f_{th}^d = 0.025\ Hz$. The MPC is carried out with control and prediction horizons $N_c = N_p = 8$. The wind profiles used in the simulations come from real measurements with 5 seconds sampling. The data were statistically processed and sent to the different machines after a spline interpolation. Figure 3 reports an example of the used profiles. For clarity, only three among these profiles are emphasized together with the estimates obtained through the local Kalman filter. Such estimates are computed using the measurements of the generators' angular speeds $\omega_{g,i}$ corrupted by zero-mean additive Gaussian noise with standard variation $\sigma_{\omega_g} = 0.01\ m/s$.

In the simulated scenario load increases the power absorption of 50 MW at 30 s. This causes a sudden decrease of the grid frequency which activates the MPC frequency support. Figure 4 depicts the grid frequency obtained with and without the WF support. It is clear that, in the former case, the frequency variation is more limited with respect to the latter standard case. Figure 4 also depicts the reference signal tracked by the MPC algorithm (more precisely

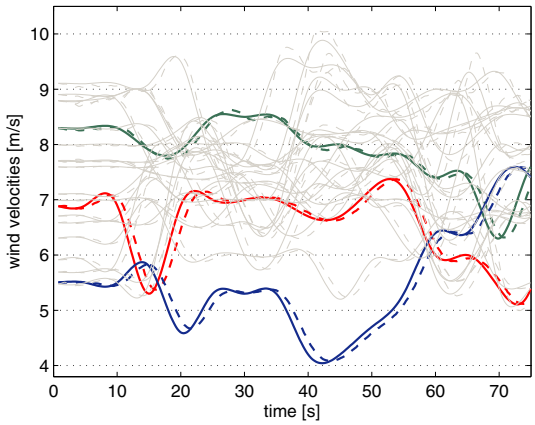

Fig. 3. Wind profiles (solid) and estimates (dashed).

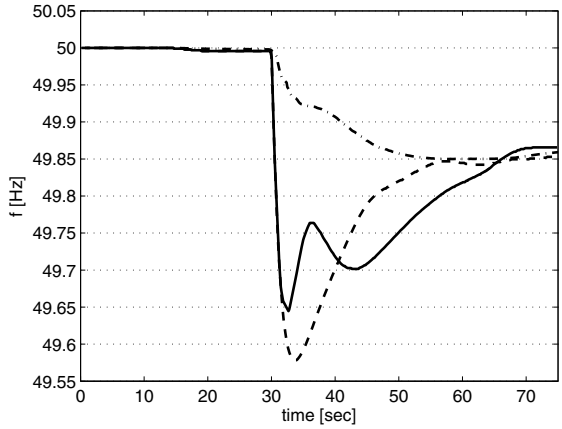

Fig. 4. Grid frequency with (solid) and without (dashed) the contribution of the WF, and frequency reference signal (dot-dashed).

the drawn signal is $\Delta f^0 + f^{nom}$, with $f^{nom} = 50\ Hz$).It is worth noting that the final value is smoothly reached thanks to a suitable choice of the state standard variation σ_L. The resulting reference signal is therefore useful to push up the frequency toward its nominal value during the first 20 seconds and to deactivate the control when the final droop is reached.

Figures 5 and 6 give details of the MPC control action. When the control is activated, an additive power is demanded to all the wind turbines, as shown in Fig. 5. This causes the temporary deceleration of the WTs as depicted in Fig. 6. For clarity, the graphs of three particular WTs with different wind conditions are emphasized. Colours in figures 3, 5 and 6 are referred to the same three WTs. As expected, the MPC control succeeds to differentiate the frequency support provided by the WTs in function of their local dynamical condition. Indeed, among the three cases emphasized in Figs. 5 and 6, the highest contribution is required to the WT which is rotating at the highest speed (green line).

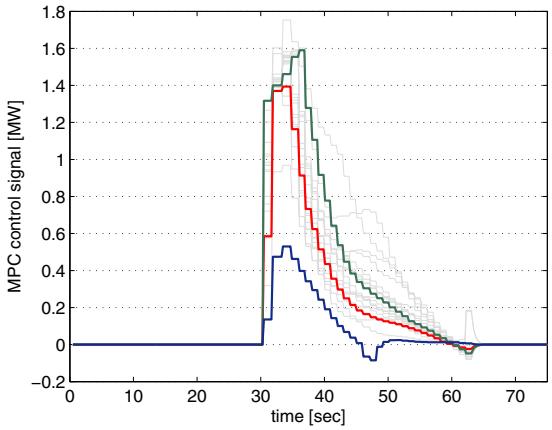

Fig. 5. MPC control signals (u_i).

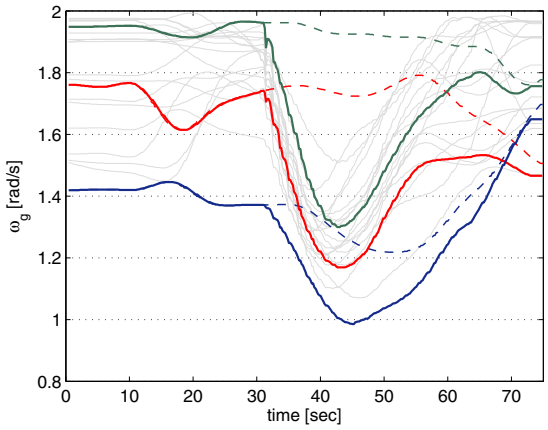

Fig. 6. WTs generator angular speeds.

5. CONCLUSIONS

The paper presents a model-based control technique to improve the contribution of wind power generators to primary frequency regulation in electric power systems. The principal aim is to suitably coordinate the control action of the single aeroturbines taking into account both dynamical and wind conditions. The results obtained from a simulated field made up of twenty wind generators shows this capability of adaptation to the current local conditions. Future works will be devoted to the study of to analyze the effects of communication delays on the control strategy.

REFERENCES

J. Aho, A. Buckspan, J. Laks, P. Fleming, Yunho Jeong, F. Dunne, M. Churchfield, L. Pao, and K. Johnson. A tutorial of wind turbine control for supporting grid frequency through active power control. In *American Control Conf. (ACC)*, pages 3120–3131, June 2012.

C. Bruno, M. Massucco, A. Pitto, M. Pozzi, M. Sforna, and F. Silvestro. An innovative pluralistic load-frequency control scheme for the power flow control along corridors on the italian border. In *IEEE PSCE*, pages 2166–2173, October 2006.

R. G. de Almeida and J. A. Peças Lopes. Participation of doubly fed induction wind generators in system frequency regulation. *IEEE Trans. Power Syst.*, 22(3): 944–950, August 2007.

I. Erlich and M. Wilch. Primary frequency control by wind turbines. In *IEEE PES Gen. Meet.*, July 2010.

DIgSILENT GmbH. *DIgSILENT PowerFactory User's Manual: Version 15.0.* 2013.

S. Grillo, M. Marinelli, F. Silvestro, F. Sossan, O. Anaya-Lara, and G. Burt. Transient support to frequency control from wind turbine with synchronous generator and full converter. In *Universities Power Engineering Conf. (UPEC)*, September 2010a.

S. Grillo, S. Massucco, A. Morini, A. Pitto, and F. Silvestro. Microturbine control modeling to investigate the effects of distributed generation in electric energy networks. *IEEE Syst. J.*, 1(3):303–312, September 2010b.

S. Grillo, M. Marinelli, S. Massucco, and F. Silvestro. Optimal management strategy of a battery-based storage system to improve renewable energy integration in distribution networks. *IEEE J. SG*, 3(2):950–958, June 2012.

H.T. Ma and B.H. Chowdhury. Working towards frequency regulation with wind plants: Combined control approaches. *Renewable Power Generation, IET*, 4(4): 308–316, July 2010.

D. Q. Mayne, J. B. Rawlings, C. V. Rao, and P. O. M. Scokaert. Constrained model predictive control: Stability and optimality. *Automatica*, 36:789–814, 2000.

A. Menichelli and A. Bemporad. Hybrid model predictive control of solar air conditioning plant. *European Journal of Control*, 14(6):501–515, 2008.

E. Muljadi, V. Gevorgian, M. Singh, and S. Santoso. Understanding inertial and frequency response of wind power plants. In *IEEE Symposium on Power Electronics and Machines in Wind Applications*, July 2012.

Wei Qiao, Wei Zhou, J.M. Aller, and R.G. Harley. Wind speed estimation based sensorless output maximization control for a wind turbine driving a dfig. *IEEE Trans. Power Electron.*, 23(3):1156–1169, May 2008.

C. Rahmann, H.-J. Haubrich, A. Moser, R. Palma-Behnke, L. Vargas, and M. B. C. Salles. Justified fault-ride-through requirements for wind turbines in power systems. *IEEE Trans. Power Syst.*, 26(3):1555–1563, August 2011.

G. Ramtharan, A. Arulampalam, J.B. Ekanayake, F.M. Hughes, and N. Jenkins. Fault ride through of fully rated converter wind turbines with ac and dc transmission. *Renewable Power Generation, IET*, 3(4):426–438, December 2009.

F. Saccomanno. *Electric Power Systems: Analysis and Control.* Wiley-IEEE Press, 2003.

A.N. Venkat, I.A. Hiskens, J.B. Rawlings, and S.J. Wright. Hybrid model predictive control of solar air conditioning plant. *IEEE Trans. Control Syst. Technol.*, 12(6):1192–1206, November 2008.

Dawei Xiang, L. Ran, P.J. Tavner, and S. Yang. Control of a doubly fed induction generator in a wind turbine during grid fault ride-through. *IEEE Trans. Energy Convers.*, 21(3):652–662, September 2006.

Y. Zong, D. Kullmann, A. Thavlov, O. Gehrke, and H.W. Bindner. Application of model predictive control for active load management in a distributed power system with high wind penetration. *IEEE Trans. Smart Grid*, 3(2):1055–1062, June 2012.